Nonlinear Dynamics (2005) 39: 95–112

A General Data-Based Approach for Developing Reduced-Order Models of Nonlinear MDOF Systems

S. F. MASRI[1,*], J. P. CAFFREY[1], T. K. CAUGHEY[2], A. W. SMYTH[3], and A. G. CHASSIAKOS[4]
[1]*School of Engineering, University of Southern California, Los Angeles, CA 90089, U.S.A.;* [2]*Division of Engineering & Applied Science, California Institute of Technology, Pasadena, CA 91125, U.S.A.;* [3]*School of Engineering & Applied Science, Columbia University, New York, NY 10027, U.S.A.;* [4]*School of Engineering, California State University, Long Beach, CA 90840, U.S.A.;* [*]*Author for correspondence (e-mail: masri@usc.edu)*

(Received: 27 September 2003; accepted: 3 March 2004)

Abstract. A general procedure is presented for analyzing dynamic response measurements from complex multi-degree-of-freedom nonlinear systems incorporating arbitrary types of nonlinear elements. The analysis procedure develops a reduced-order, nonlinear model whose format is convenient for numerical simulation studies. No information about the system's mass properties is needed, and only the applied excitations and corresponding response are needed to develop the model whose dimension is compatible with the number of available sensors. The utility of the approach is demonstrated by means of a three-degree-of-freedom system incorporating polynomial-type nonlinear features with hardening as well as softening characteristics.

Key words: identification, modeling, nonlinear systems, simulation, validation

1. Introduction

1.1. Motivation

There is a lot of interest in developing accurate data-based models of complex, nonlinear, multi-degree-of-freedom (MDOF) systems whose underlying nature is not easily identified (i.e., where the model class is not obvious). This interest stems from basic modeling needs for several application types. For example, for a variety of simulation purposes it is important to obtain data-based models which capture the phenomenological behavior of complex dynamic processes. Another example is the area of vibration control and suppression which relies on having accurate process ("plant") modeling. Lastly, for health monitoring and damage detection of structural and mechanical systems based on their vibration response characteristics, system change (or damage) can be inferred from changes in identified model parameters. A few sample publications focusing on challenging issues in the modeling and identification of nonlinear systems include the work of Mohammad et al. [1], Housner et al. [2], Ghanem and Romeo [3], Worden and Tomlinson [4], and Vestroni and Noori [5].

The authors have previously developed a multi-stage approach for "fitting" the nonlinear system excitations in a nonparametric form (Masri et al. [6]). The term *nonparametric* here distinguishes the approach from a *parametric* approach where model *parameters* are directly related to physical or phenomenological quantities. In the present paper, this nonparametric approach is generalized so that no information is assumed about the system mass; the needed system inertia properties are directly identified by the new method of this paper. Furthermore, there is a significant improvement from the computational point of view since the nonparametric representation of the system's accelerations is performed for one acceleration component at a time. Furthermore, by "rotating" the reduced-order

system coordinates in the "modal" space of each particular problem, a major reduction is achieved in the complexity of the system components needed to represent the dominant system response nonlinearities.

1.2. Scope

Section 2 presents the formulation of the proposed identification approach; Section 3 applies the approach to a generic nonlinear three-degree-of-freedom (3DOF) system under un-correlated stationary random excitation, and Section 4 validates the modeling results by predicting the nonlinear system response under the action of a single, mass-proportional, non-stationary excitation. Section 5 presents a discussion of pertinent issues such as effects of measurements noise pollution, trade-offs in model-order reduction and complexity, and effects of memory-type (hysteretic) nonlinearities.

2. Formulation

2.1. Equation of Motion

Consider a discrete MDOF system which is subjected to directly applied excitation forces $\underline{f}(t)$. The motion of this multi-input/multi-output nonlinear system is assumed to be governed by the set of equations

$$M\underline{\ddot{x}}(t) + C\underline{\dot{x}}(t) + K\underline{x}(t) + \underline{f}_{\mathrm{N}}(t) = \underline{f}(t), \tag{1}$$

where, $\underline{f}(t)$ = an n column vector of directly applied forces, $\underline{x}(t)$ = displacement vector of order n, M, C, K = constant matrices that characterize the inertia, linearized damping, and linearized stiffness forces, $\underline{f}_{\mathrm{N}}(t)$ = vector of nonlinear nonconservative forces.

In the method under discussion, the linear parametric part of the class of models defined above is first identified by using a time-domain method for the identification of the equivalent linear system matrices appearing in Equation (1). This can be accomplished by expressing the acceleration vector in the form

$$\underline{\ddot{x}}(t) = -M^{-1}C\underline{\dot{x}}(t) - M^{-1}K\underline{x}(t) + M^{-1}\underline{f}(t), \tag{2}$$

in which the ith component of $\underline{\ddot{x}}$ is given by:

$$\ddot{x}_i(t) = \sum_{j=1}^{n} a_{ij}\dot{x}_j(t) + \sum_{j=1}^{n} b_{ij}x_j(t) + \sum_{j=1}^{n} c_{ij}f_j(t), \quad (i = 1, 2, \ldots, n). \tag{3}$$

Using standard least-squares techniques, the algebraic coefficients (elements of the unknown system matrices) can be identified.

Subsequently, the contribution of the unknown nonlinear forces can be found from

$$M^{-1}\underline{f}_{\mathrm{N}}(t) = -\underline{\ddot{x}}(t) - M^{-1}C\underline{\dot{x}}(t) - M^{-1}K\underline{x}(t) + M^{-1}\underline{f}(t). \tag{4}$$

Notice that the terms appearing on the left-hand-side of Equation (4) represent the residual (nonlinear) acceleration components that could not be expressed as a linear functions of the system state variables and the corresponding excitations.

2.2. Nonlinear Nonparametric Terms

Rather than attempt to determine an approximating analytical expression for each component of $M^{-1}\underline{f}_{\mathrm{N}}(t)$, experience has shown that a much more efficient approach (especially when there is a large number of degrees of freedom to consider), is to "rotate" the system coordinates by using the eigenvectors corresponding to the linearized system matrices, in order to obtain the transformed nonlinear accelerations:

$$\underline{h}(t) = \Phi^T M^{-1}\underline{f}_{\mathrm{N}}(t), \tag{5}$$

where ϕ is the eigenvector matrix associated with $M^{-1}K$.

Let $h_i(t)$ represent the ith component of the transformed nonlinear residual acceleration vector as defined by Equation (5). In general, vector $\underline{h}$ depends simultaneously on all the components of the system's velocity and displacement vectors:

$$\underline{h}(t) = \underline{h}(\underline{x}, \underline{\dot{x}}). \tag{6}$$

The central idea of the present method (Masri and Caughey, 1979) is that, in the case of nonlinear dynamic systems commonly encountered in the structural mechanics field, a judicious assumption is that each component of $\underline{h}$ can be expressed in terms of a series of the form:

$$h_i(\underline{x}, \underline{\dot{x}}) \approx \sum_{j=1}^{J_{\max_i}} \hat{h}_i^{(j)}\left(q_{1_i}^{(j)}, q_{2_i}^{(j)}\right) \tag{7}$$

where the q_1's and q_2's are suitable generalized coordinates which, in turn, are linear combinations of the physical displacements, velocities. The approximation indicated in Equation (7) is that each component h_i of the transformed nonlinear (residual) acceleration vector $\underline{h}$ can be adequately estimated by a collection of terms $\hat{h}_i^{(j)}$ each one of which involves a pair of generalized coordinates. The particular choice of combinations and permutations of the generalized coordinates and the number of terms $J_{\max_i}$ needed for a given h_i depends on the nature and extent of the nonlinearity of the system and its effects on the specific DOF i.

If $h_i(t)$ is chosen as the ith component of $\underline{f}_{\mathrm{N}}(t)$, then the procedure expressed by Equation (7) will directly estimate the corresponding component of the unknown nonlinear force. For certain structural configurations (e.g., localized nonlinearities) and/or relatively low-order systems, the choice of suitable generalized coordinates for the series in Equation (7) is a relatively straightforward task. However, in many practical cases involving distributed nonlinearities coupled with a relatively high-order system, an improved rate of convergence of the series in Equation (7) can be achieved by performing the least-squares fit of the nonlinear accelerations in the "modal" domain as outlined below.

Using the identification results for the linear part, the eigenvalue problem associated with $M^{-1}K$ is solved resulting in the eigenvector or modal matrix Φ and the corresponding vector of generalized coordinates $\underline{u}$:

$$\underline{h}(\underline{u}, \underline{\dot{u}}) = \Phi^T M^{-1}\underline{f}_{\mathrm{N}}(t) \tag{8}$$

with

$$\underline{u}(t) = \Phi^{-1}\underline{x}(t) \tag{9}$$

With this formulation in mind, Equation (7) can be viewed as allowing for "modal" interaction between all generalized coordinates, taken two at a time. Note that the formulation in Equation (7) allows for "modal" interaction between all "modal" displacements, velocities and accelerations.

3. Application

3.1. Example Nonlinear 3DOF Model Characteristics

To illustrate the application of the method under discussion, consider the example of finite element model shown in Figure 1. This one-dimensional structure (rectlinear horizontal motion) consists of three nearly equal masses $m_i, i = 1, 2, 3$ that are interconnected by means of six truss elements anchored to an interface at three locations, thus resulting in a redundant system with three degrees of freedom. Notice that the structure of the system is not chain-like, consequently, the linearized system stiffness matrix is not banded.

The absolute displacement of each m_i is designated by x_i while the three excitation forces that directly act on this system are denoted by $f_i(t), i = 1, 2, 3$. Thus

$$\underline{x}(t) = \{x_1, x_2, x_3\}^{\mathrm{T}}, \tag{10}$$

$$\underline{f}(t) = \{f_1, f_2, f_3\}^{\mathrm{T}}. \tag{11}$$

The arbitrary nonlinear elements, denoted by g_i, that are interposed between the masses and between the support points are dependent on the relative displacement y and the velocity $\dot{y}$ across the terminals of each element. In the case of polynomial nonlinearities, the elements assume the form,

$$g_i(y, \dot{y}) = p_1^{(i)} y + p_2^{(i)} \dot{y} + p_3^{(i)} y^3, \tag{12}$$

where $p_1^{(i)}$ is the linear stiffness component, $p_2^{(i)}$ is the linear viscous damping term, and $p_3^{(i)}$ corresponds to the coefficient of the nonlinear (cubic) displacement term. Thus, depending on the sign of $p_3^{(i)}$, the form of g_i in Equation (12) can be made to represent restoring forces with hardening or softening nonlinearities – a commonly encountered type of nonlinearity in physical systems.

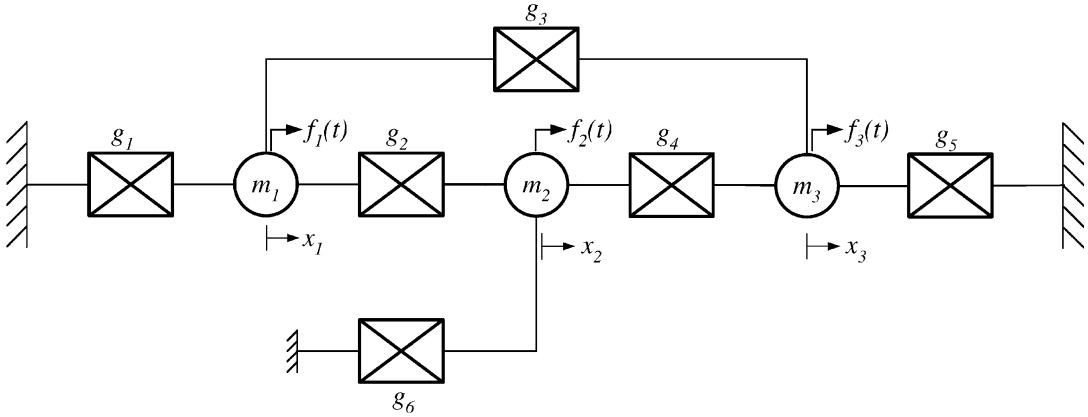

Figure 1. Model of nonlinear 3DOF system used to generate synthetic data.

Table 1. Nonlinear element properties.

Element index i	$p_1^{(i)}$	$p_2^{(i)}$	$p_3^{(i)}$
1	39.478	0.628	+19.739
2	39.478	0.628	−19.739
3	39.478	0.628	−19.739
4	39.478	0.628	−19.739
5	39.478	0.628	+19.739
6	39.478	0.628	+19.739

The magnitude of the system masses were: $m_1 = 0.8$, $m_2 = 2.0$, and $m_3 = 1.2$. The material properties of the nonlinear model elements are shown in Table 1.

3.2. Nonlinear System Response Under Random Force Excitation

The method under consideration imposes no restrictions on the nature of the excitation source to be used as a probing signal. It will be assumed in the present example that three uncorrelated broad-band random excitations are applied to the three system masses, with each force corresponding to a stationary random process having zero mean and a standard deviation σ_i, with $\sigma_1 = 20.0, \sigma_2 = 20.0$ and $\sigma_3 = 20.0$.

Figure 2 shows the excitation forces over a time period covering approximately 20 fundamental periods of the linearized system. Notice that the excitations are indeed uncorrelated and are relatively broad-band in nature.

The response of this system over a period of about $10T$ is shown in Figure 3, in which the left-hand-side (LHS) column shows the time history of the system displacements x_1, x_2, and x_3, the middle column shows the corresponding system velocities, and the RHS column shows the corresponding system accelerations, all covering a time period of about $20T_1$.

The time histories of the six nonlinear element forces $g_i(t)$ are shown in Figure 4.

Phase-plane plots of all the elements' force-deformation curves are shown in Figure 5, where it is clear that elements g_1, g_5 and g_6 have a hardening–spring characteristic, while elements g_2, g_3 and g_4 have a softening–spring characteristic. It is worth noting that while the individual element deformation characteristics are "measured" and plotted in this example, such quantities in general are not accessible for measurements, due to the non-chain nature of arbitrary systems where interaction forces between oscillating masses have simultaneous contributions from multiple (redundant) structural members. In the method under discussion, no information about the nature of element forces is utilized in the analysis. The member forces are being shown here to demonstrate that the system is indeed undergoing significant nonlinear deformations.

3.3. Identification of Linear Acceleration Terms

Using the identification method under discussion, and selecting as basis vectors a linear combinations of all the degrees-of-freedom in the system's displacement, velocity, and excitation

$$\text{basis} = \{d_1, d_2, d_3, v_1, v_2, v_3, f_1, f_2, f_3\} \tag{13}$$

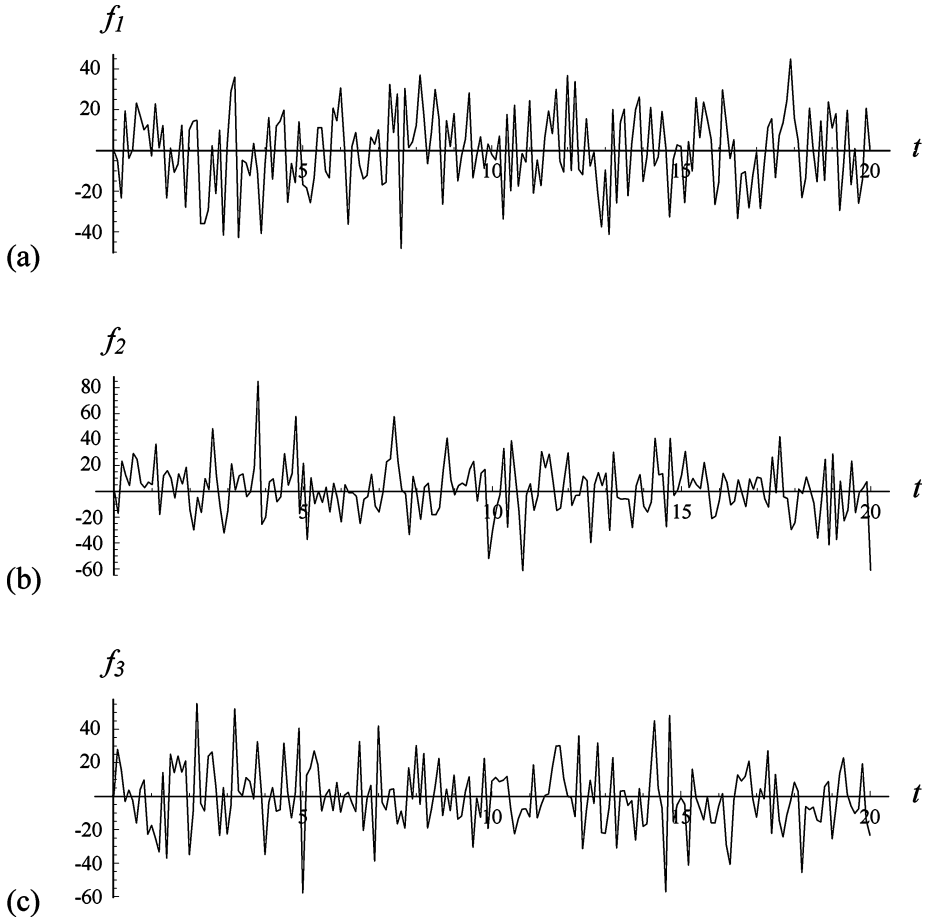

Figure 2. Nonlinear 3DOF system uncorrolated random excitations used for identification.

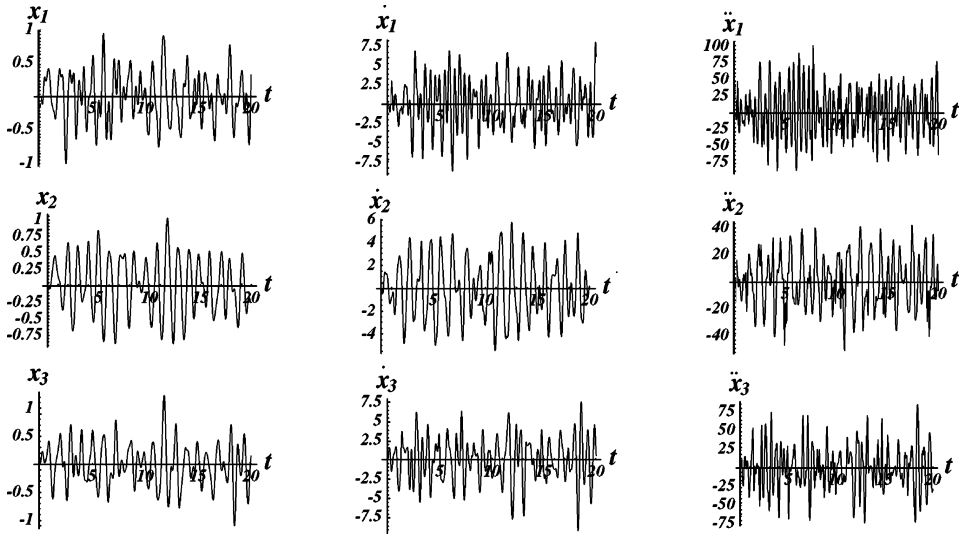

Figure 3. Nonlinear 3DOF system response data used for identification; the LHS column shows $x_i(t)$, the middle column shows $\dot{x}_i(t)$ and the RHS column shows $\ddot{x}_i(t)$.

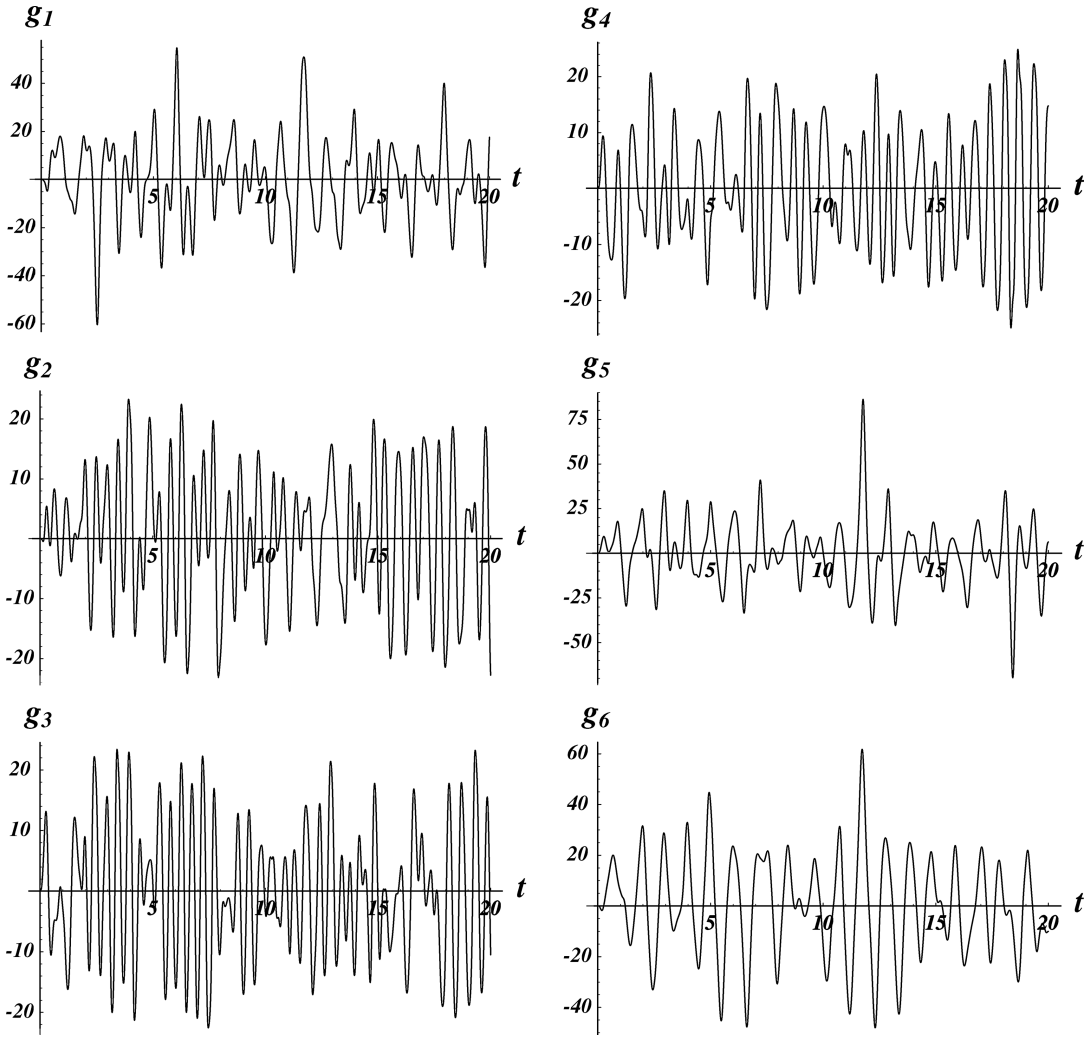

Figure 4. Nonlinear element force time histories.

results in the acceleration response of m_1 being estimated by:

$$\begin{aligned}\hat{\ddot{x}}_1 = &-144.554\, d_1 + 44.5965\, d_2 + 42.3514\, d_3 \\ &+ 1.21716\, f_1 + 0.0156361\, f_2 + 0.00813426\, f_3 \\ &- 2.27221\, v_1 + 0.839124\, v_2 + 0.665058\, v_3 \end{aligned} \tag{14}$$

Similarly, the least squares fit yields for the estimated acceleration $\hat{\ddot{x}}_2$ for mass m_2:

$$\begin{aligned}\hat{\ddot{x}}_2 = &\ 17.5801\, d_1 - 57.7158\, d_2 + 16.1263\, d_3 \\ &- 0.00421075\, f_1 + 0.500484\, f_2 - 0.0087248\, f_3 \\ &+ 0.306268\, v_1 - 0.965233\, v_2 + 0.315172\, v_3 \end{aligned} \tag{15}$$

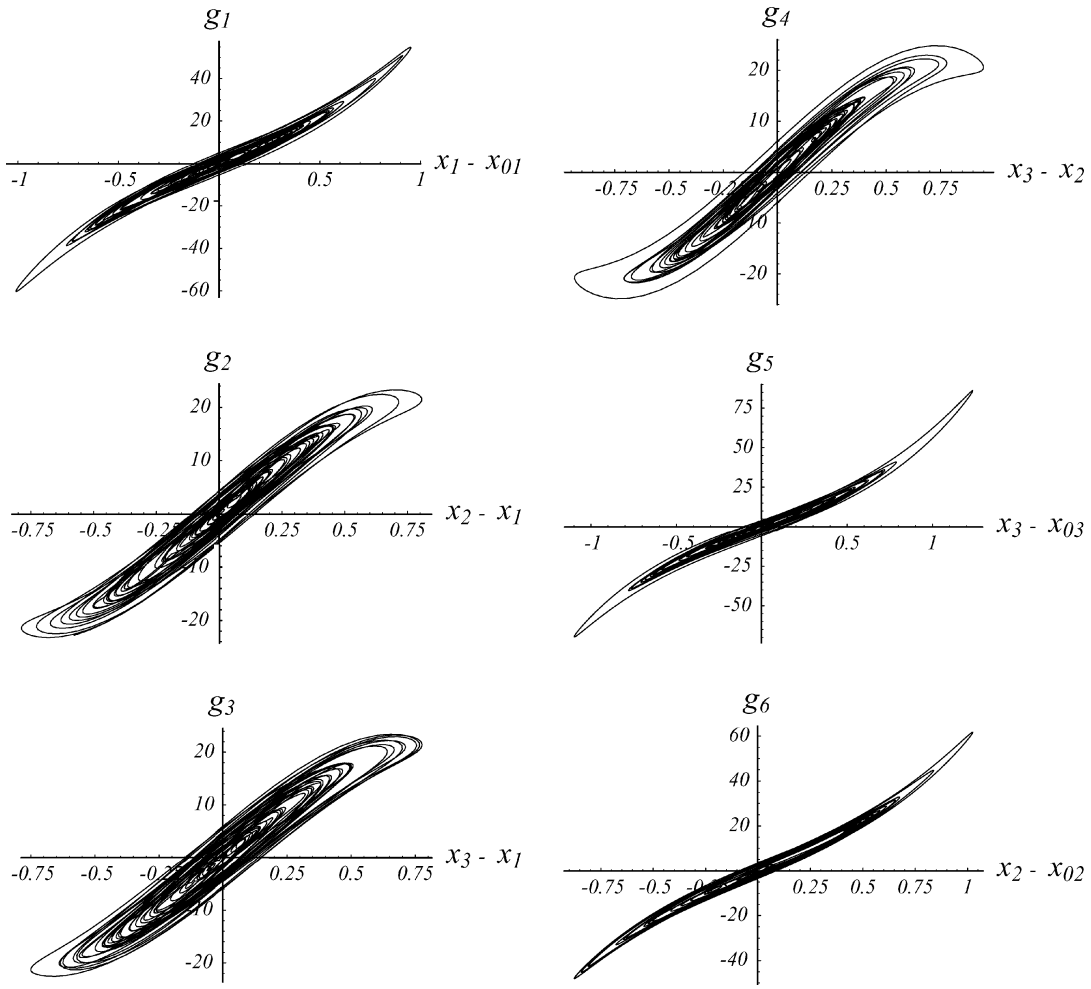

Figure 5. Phase diagram of nonlinear elements.

and the estimated acceleration for $\hat{\ddot{x}}_3$ for m_3:

$$\begin{aligned}\hat{\ddot{x}}_3 = {} & 28.6254\, d_1 + 28.9007\, d_2 - 96.9454\, d_3 \\ & - 0.00556618\, f_1 + 0.00524687\, f_2 + 0.793694\, f_3 \\ & + 0.571428\, v_1 + 0.435982\, v_2 - 1.50858\, v_3 \end{aligned} \tag{16}$$

A graphical representation of the accuracy of the identification results is shown in Figure 6, in which the left-hand-side column of plots shows the time history of the three identified system accelerations $\hat{\ddot{x}}_1$, $\hat{\ddot{x}}_2$, and $\hat{\ddot{x}}_3$, while the RHS panel of plots corresponds to the residual accelerations r_i found by subtracting the linearized term from the "measured" signals: $r_i = \hat{\ddot{x}}_i - \ddot{x}_i$. For ease of comparison, identical time and amplitude scales are used for all the plots displayed in Figure 6. It should be noted that the least-squares approximations of the three acceleration responses here were obtained using time-histories containing 1000 time samples.

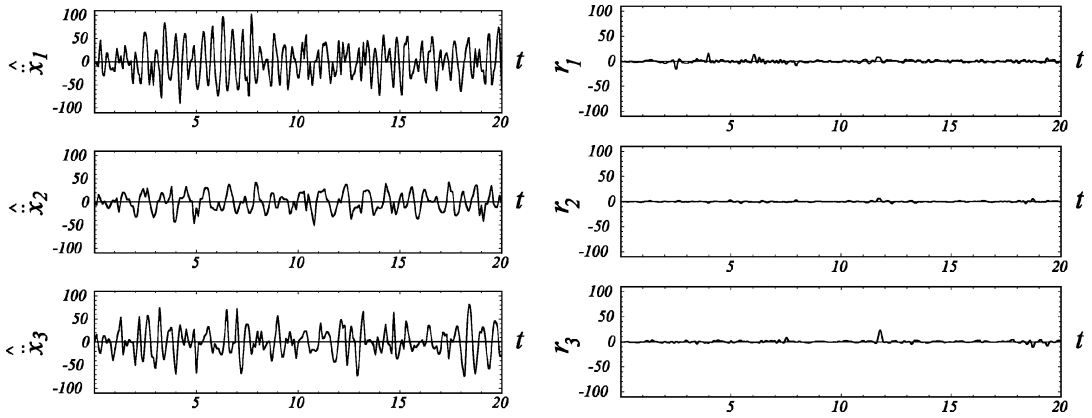

Figure 6. Comparison of estimated accelerations $\hat{\ddot{x}}_i$ and residual accelerations $r_i = \hat{\ddot{x}}_i - \ddot{x}_i$. For convenience, identical scales are used for all plotted quantities.

3.4. Identification of Linearized System Matrices

Noting that the identified coefficients of the excitation components correspond to the elements of the inverse mass matrix, then the identified matrix M^{-1} is found to be (rounded to three significant digits):

$$M^{-1} = \begin{pmatrix} 1.217 & 0.016 & 0.008 \\ -0.004 & 0.500 & -0.009 \\ -0.006 & 0.005 & 0.794 \end{pmatrix} \tag{17}$$

from which the identified system mass matrix can be determined:

$$M = \begin{pmatrix} 0.821 & -0.026 & -0.009 \\ 0.007 & 1.998 & 0.022 \\ 0.006 & -0.013 & 1.260 \end{pmatrix} \tag{18}$$

Based on the system parameters used in the example problem, the exact system mass matrix should be:

$$M_{\text{exact}} = \begin{pmatrix} 0.80 & 0.0 & 0.0 \\ 0.0 & 2.0 & 0.0 \\ 0.0 & 0.0 & 1.2 \end{pmatrix} \tag{19}$$

Clearly, the identified system matrix M is very close to the exact one.

By using the identified system accelerations in Equations (14)–(16), and recognizing that the coefficients of the velocity to the first power terms are elements of $M^{-1}C$, leads to the identified system (equivalent linear) damping matrix:

$$C = \begin{pmatrix} 1.879 & -0.710 & -0.551 \\ -0.608 & 1.913 & -0.601 \\ -0.703 & -0.567 & 1.900 \end{pmatrix} \tag{20}$$

Similarly, by using the identified system accelerations in Equations (14–16), and recognizing that the coefficients of the displacement to the first power terms are elements of $M^{-1}K$, leads to the identified system (equivalent linear) stiffness matrix:

$$K = \begin{pmatrix} 119.444 & -37.858 & -35.221 \\ -34.731 & 114.349 & -30.389 \\ -34.999 & -37.434 & 122.098 \end{pmatrix} \tag{21}$$

Notice that, even though no assumptions were made in the formulation of the data processing scheme concerning the nature of the system matrices, the identified (equivalent linear) damping and stiffness matrices are nearly symmetric.

3.5. Identification of Linearized System "Modal" Matrix

Now using the identified system matrices listed above, yields an estimate of the linearized system "modal" properties. The normalized eigenvectors obtained from solving the eigenvalue matrix associated with $M^{-1}K$ is

$$\Phi = \begin{pmatrix} 1. & 1. & 1. \\ -0.107 & -1.312 & 1.446 \\ -0.374 & 2.415 & 1.105 \end{pmatrix} \tag{22}$$

with the three identified frequencies (in Hz) being $\omega = \{2.045, 1.598, 0.917\}$.

Furthermore, with the identified system mass, damping and stiffness matrices having been found, the damped system frequencies and corresponding ratios of critical damping can be directly computed by determining the eigenvalues of the system state matrix. The ability to construct the equivalent linear system matrices is a useful by-product of the data processing approach under discussion. In some cases, this may be the end result that is desired, and no further identification tasks need be implemented.

3.6. Transformed Nonlinear Residual Accelerations

Using the modal matrix Φ to "rotate" the coordinates from configuration space to modal space, and applying the transformations indicated in Equation (5) and Equation (9) yields the time history of the transformed generalized coordinates $u_i(t)$ and the corresponding transformed nonlinear residual accelerations $h_i(t)$.

The left-hand-side panel of plots shown in Figure 7 corresponds to the time histories of $u_1(t)$, $u_2(t)$, and $u_3(t)$, using the same time segment, but having different amplitude scales for each plot. Note that, not surprisingly, mode number 3 (the one associated with the lowest frequency) has the largest magnitude.

On the RHS panel of Figure 7 is shown individual phase-plots of each transformed nonlinear acceleration versus the corresponding generalized displacement. For better resolution, different scales are used for the abscissas and ordinates of the indicated phase diagrams. The complex (nonlinear) dependence of the residual accelerations on the corresponding state variable is clearly evident from inspection of the phase plots.

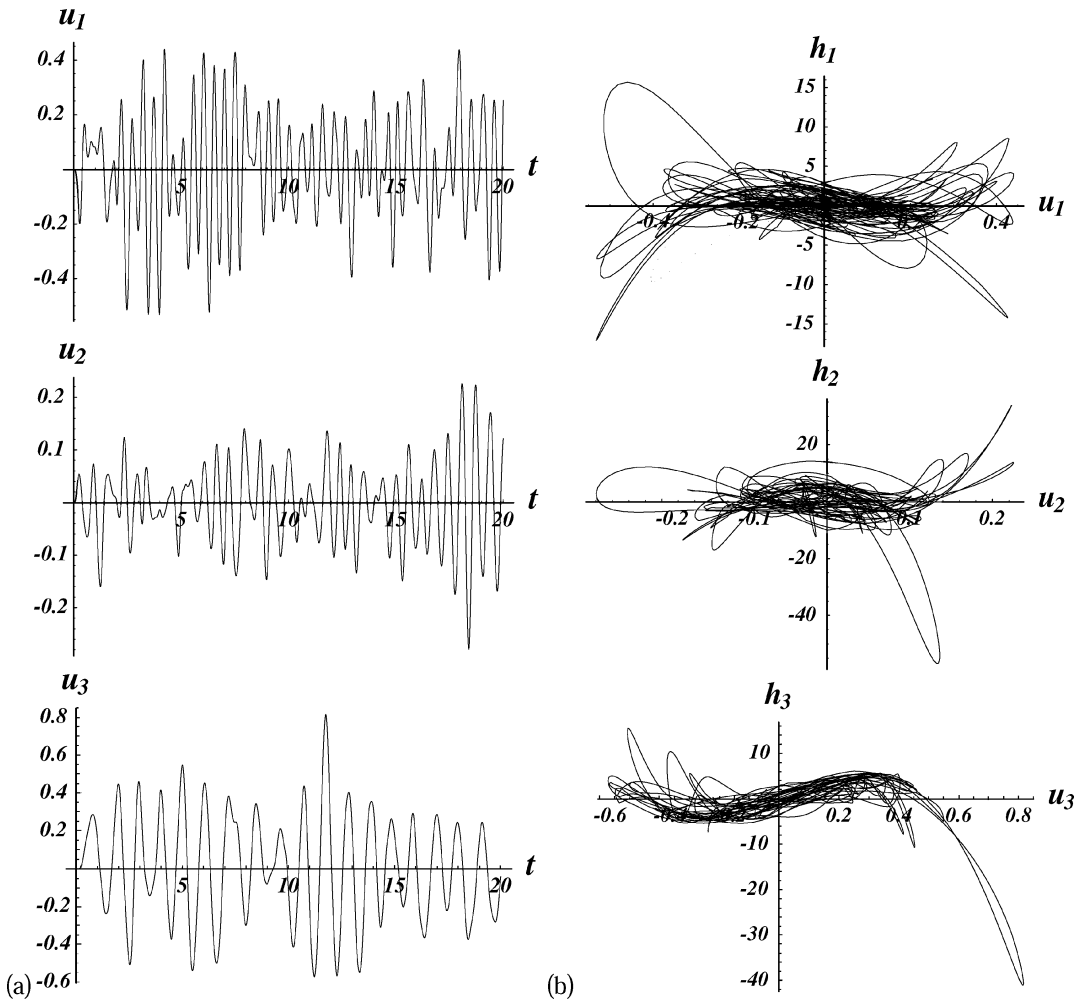

Figure 7. Transformed generalized coordinates and phase diagram of transformed nonlinear acceleration.

3.7. Power Series Fit of Transformed Nonlinear Accelerations

Selecting values for the order $j_{\max} = 3$ of the basis functions in Equation (7) results in the following basis:

$$\text{basis} = \{1, v, v^2, v^3, d, d\,v, d\,v^2, d\,v^3, d^2, d^2\,v, d^2\,v^2, d^2\,v^3, d^3, d^3\,v, d^3\,v^2, d^3\,v^3\} \tag{23}$$

By fitting the transformed nonlinear residual acceleration term $h_3(t)$ as indicated in Equation (7), results in the following expression, where for convenience, the term d corresponds to the modal displacement u_3, and the term v corresponds to the modal velocity $\dot{u}_3$:

$$\begin{aligned}\hat{h}_3(d, v) = {} & 0.667763 - 5891.21\,d - 199327.0\,d^2 + 2.28625 \times 10^6\,d^3 + 48.3641\,v \\ & - 10302.6\,d\,v + 1.48498 \times 10^6\,d^2\,v - 1.31112 \times 10^7\,d^3\,v + 1140.54\,v^2 + 14578.3\,d\,v^2 \\ & - 2.58127 \times 10^6\,d^2\,v^2 + 2.24354 \times 10^7\,d^3\,v^2 - 1123.1\,v^3 + 1191.81\,d\,v^3 \\ & + 1.36468 \times 10^6\,d^2\,v^3 - 1.22186 \times 10^7\,d^3\,v^3 \end{aligned} \tag{24}$$

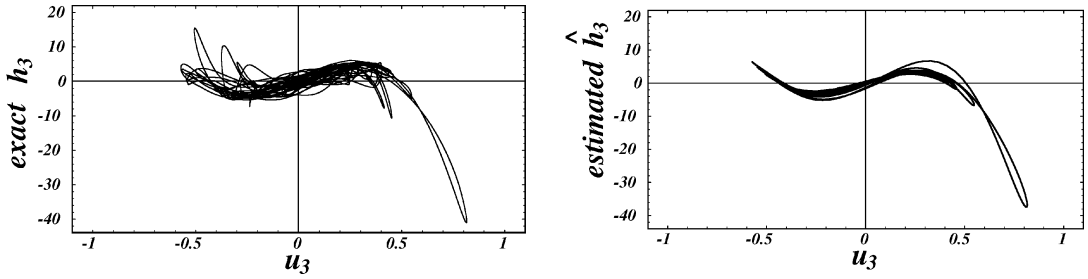

Figure 8. Phase comparison of transformed nonlinear residual acceleration $h3$.

The plots shown in Figure 8 compare the adequacy of the analytical expression in Equation (24) to estimate the nonlinear residual terms associated with "mode" number three. The LHS of Figure 8 shows a phase diagram of h_3 versus u_3, while the RHS phase plot is a corresponding phase plot of $\hat{h}_3$ versus u_3, using identical scales as used in the LHS plot. Notice the obvious cubic dependence of the "modal" acceleration term on the corresponding modal displacement. It is obvious from Figure 8 that the expression of Equation (24) provides a reasonably accurate estimate of the exact force, both qualitatively as well as quantitatively.

4. Validation

4.1. Generation of Validation Measurements

To demonstrate the utility of the identification approach under discussion to provide fairly accurate models of a tested article that can subsequently be used to predict the response of the test article under a dynamic environment that differs from the signals used to identify it, a new data set was generated from the exact nonlinear model by subjecting it to three correlated random force excitations. The same generic random excitation was amplitude-scaled by the magnitude of the mass of each system degree of freedom. This was meant to emulate a situation in which the test system is now subjected to a broad-band uniform base excitation; hence, the induced inertia loads are each proportional to the corresponding mass.

The applied system excitation in this case is shown in Figure 9, where careful inspection shows that the three forces are indeed correlated and have magnitudes that are mass-proportional.

The time histories of the exact nonlinear system displacements, velocities and accelerations under the excitations shown in Figure 9 are presented in Figure 10, where, for added resolution, different amplitude scales are used for the various displayed time histories.

Figure 11 shows a plot of the time histories of the nonlinear forces induced in all six members during this validation test, while the corresponding phase diagrams of all the nonlinear member forces versus the corresponding relative motion across each member are shown in Figure 12. Here again, the nonlinear behavior of some of the elements is clearly evident.

4.2. Comparison of Validation Results

Now using the approximating analytical expressions for $\hat{a}_1$, $\hat{a}_2$ and $\hat{a}_3$ shown in Equations (14)–(16), in conjunction with the power-series fit shown in Equation (24) for estimating the contribution of a single nonlinear "mode" $\hat{h}_3$, provides a computationally convenient form to simulate the response of the identified system when subjected to the same validation excitation shown in Figure 9.

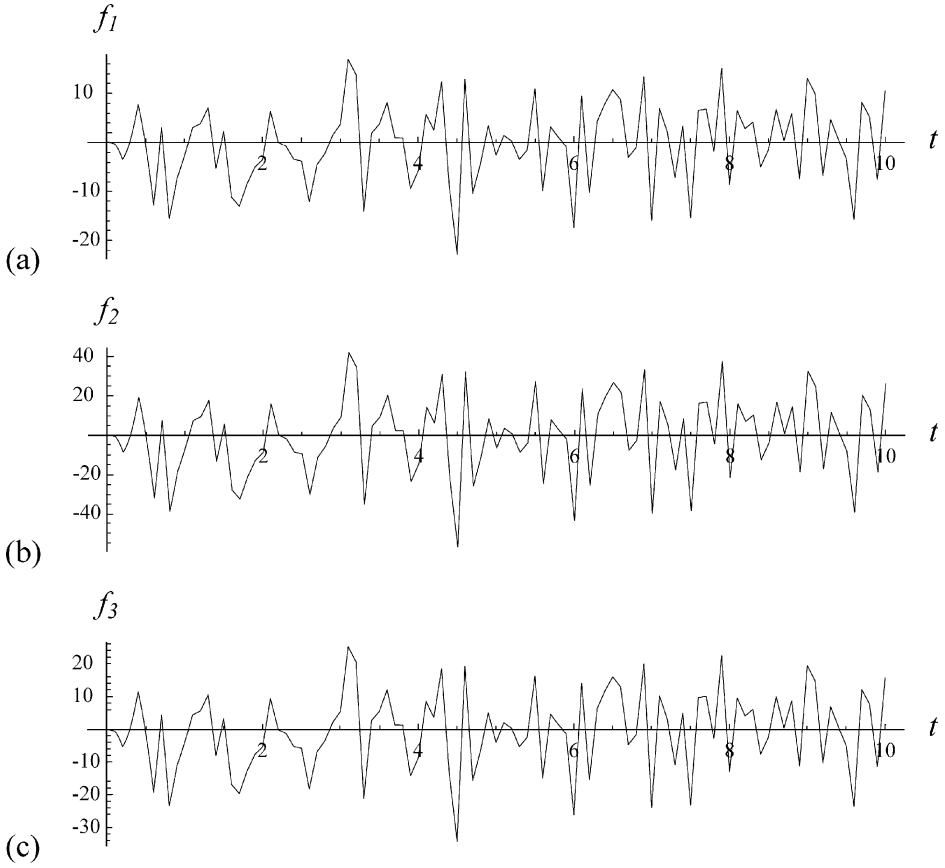

Figure 9. Nonlinear 3DOF system mass-proportional and correlated random excitations used for validation.

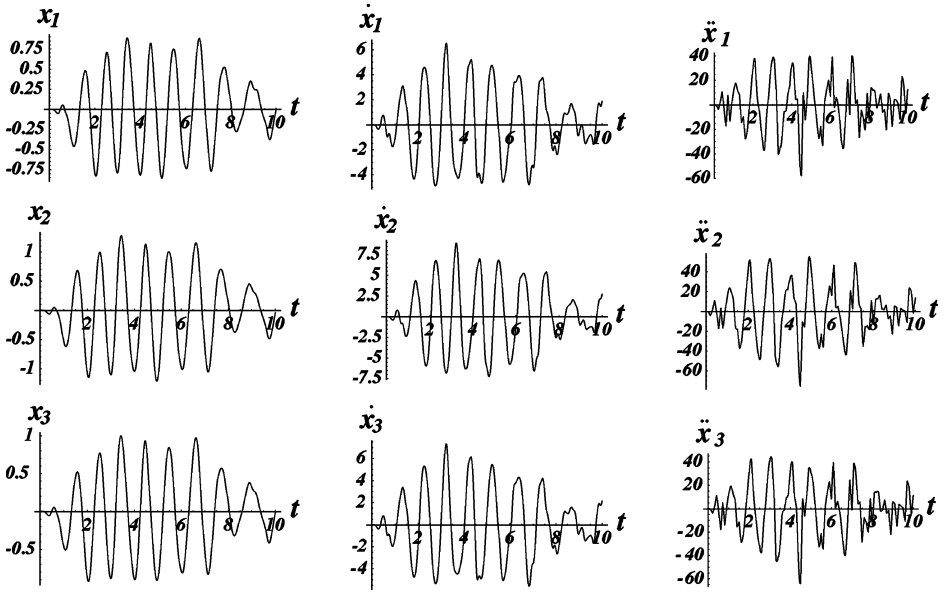

Figure 10. Nonlinear 3DOF system response data used for validation; the LHS column shows $x_i(t)$, the middle column shows $\dot{x}_i(t)$ and the RHS column shows $\ddot{x}_i(t)$.

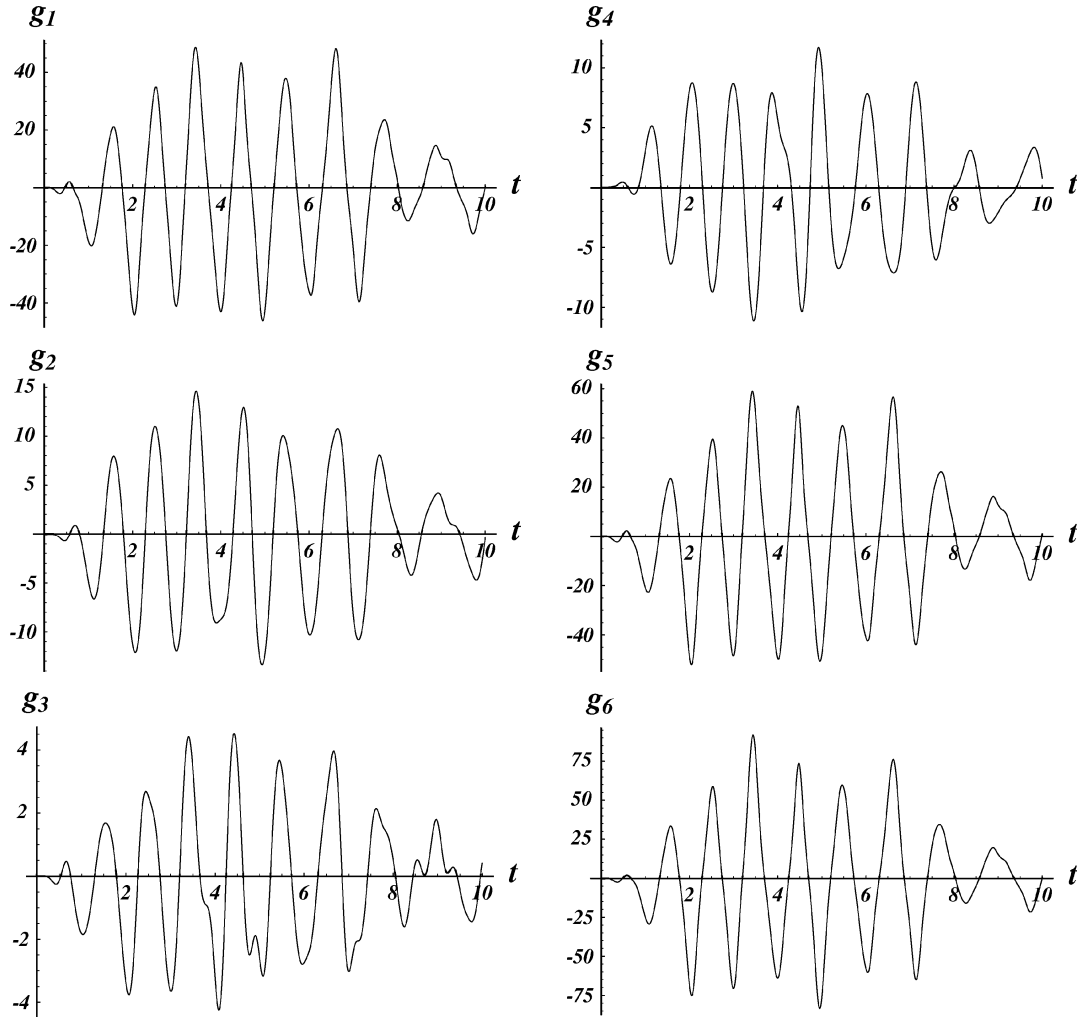

Figure 11. Validation nonlinear element force time histories.

Using standard time-marching techniques for the solution of initial-value problems, results in the simulated system response. A comparison of the exact nonlinear system acceleration (shown in the RHS panel of plots in Figure 10) with the predicted acceleration is shown in Figure 13. Note that there are three curves shown in Figure 13: the solid line represents the "exact" acceleration $\ddot{x}_2$ of m_2, the superposed long-dashed line shows the combined contribution of the linear and nonlinear terms to the estimated (predicted) $\hat{\ddot{x}}_2$, and the short-dashed line indicates the contributions of the nonlinear terms associated with h_3.

As one would expect, the nonlinear component of the response increases in magnitude with the system response level. Furthermore, while the contribution of the nonlinear terms is small relative to the linear ones, the nonlinear components do have a significant (beneficial) effect on the accuracy of the predicted solution. Note again, that because one of the goals of this study is model order reduction, that the nonlinearity in the validation model stems from only one (the most dominant) of the three nonlinear "modal" contributions. Increased accuracy could be obtained by including models of the additional transformed nonlinear residual modal contributions.

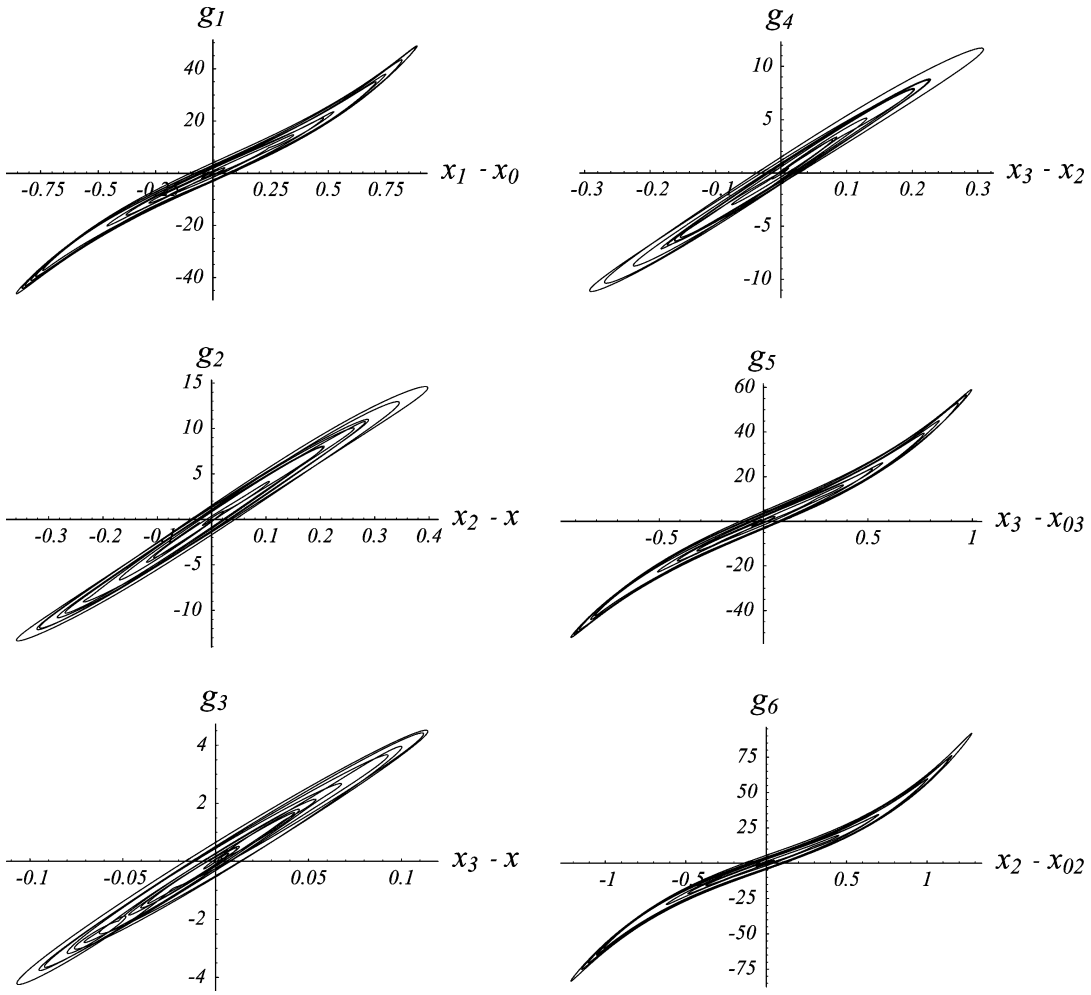

Figure 12. Validation phase diagrams of nonlinear elements.

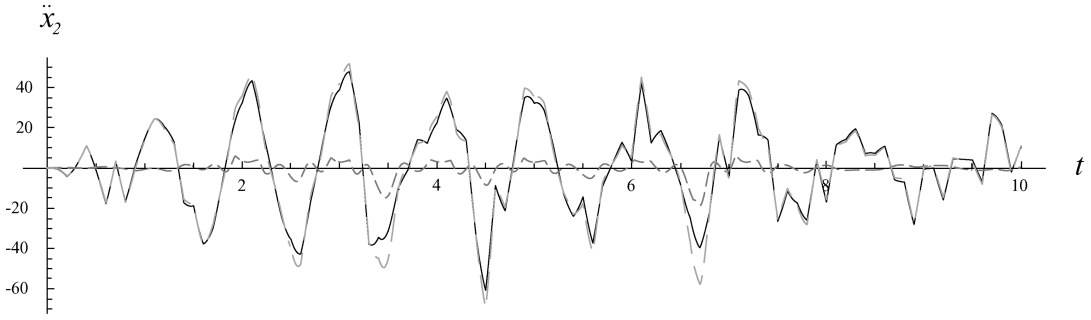

Figure 13. Validation contributions to $\ddot{x}_2$ of linear and nonlinear terms.

A comparison between the exact and estimated velocity and displacement of mass m_2 are shown in Figures 14 and 15, respectively. In each case, the solid line represents the exact response, while the dashed curve corresponds to the predicted response. Similar results are achieved for the response of m_1 and m_3.

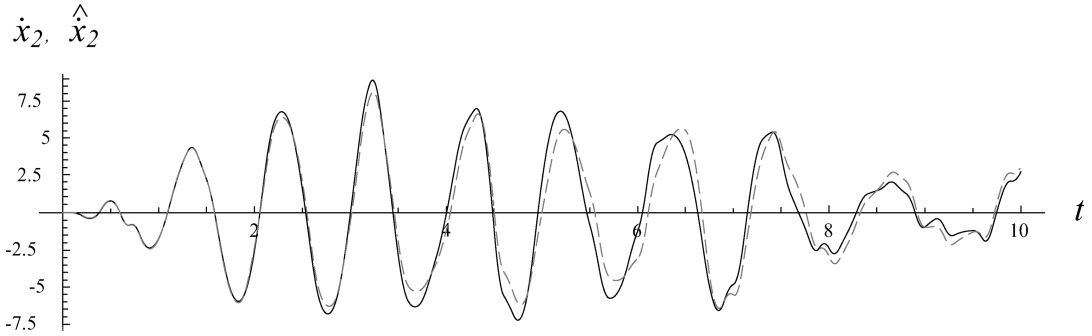

Figure 14. Comparison of exact (solid line) and predicted (dashed line) velocity $\dot{x}_2$ corresponding to the validation case.

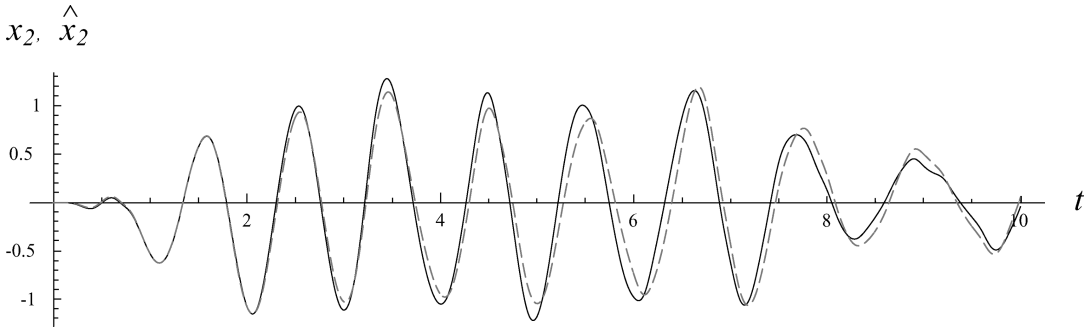

Figure 15. Comparison of exact (solid line) and predicted (dashed line) displacement x_2 corresponding to the validation case.

5. Discussion

In the present study, the "measurements" used for identification and validation were assumed noise-free; this is clearly an idealization of real-life situations. However, due to the least-squares nature of the identification scheme, broad-band noise effects tend to be "averaged out." Assuming that direct measurements are obtained of the state variables needed for identification, then the approach under discussion should be quite robust in the presence of noise pollution. However, if acceleration signals are to be used to obtain through integration the corresponding velocities and displacements, care should be taken in processing the measurements. The integration sequence of noisy signals introduces noise amplification effects (particularly low-frequency noise amplification), which distort the velocity and displacement estimates. This effect causes parameter bias and error in the associated coefficients in the model (see, for example, Worden [7]; Smyth and Pei [8]).

While the illustrative example shown in this paper was not of a large enough order to show the strong potential of the proposed modeling scheme for model-order reduction, it is worth pointing out that the more complex that the underlying nonlinear system becomes, the more useful would the approach become in developing a low-order, low-complexity nonlinear model that captures the dominant features of the exact nonlinear system behavior over the range of test excitations used as probing signals. While a higher-order of the nonlinear power-series fit of the residual nonlinear accelerations may lead to improved accuracy, this should be balanced with the accompanying added complexity (and numerical simulation additional cost).

It is also worth pointing out that the basis functions used in the fit of the residual nonlinear forces were based on using combinations of power-series terms (see Equation (24)). Since the nonlinear members used in this study had polynomial-like nonlinearities, the power-series used in the identification procedure would have some terms that are directly related to the nature of the presumably unknown nonlinearities. However, if the underlying system nonlinearities involve hysteretic type behavior with "memory" effects, then such nonlinearities could not be correctly represented by combinations of polynomials. In such situations, the proposed method would give an average mean-square fit of the response over the observation period used to model the system behavior.

Lastly, it should be noted that one could approach the system modeling using a slightly different sequence of approximation steps. Namely, one could use the same linear system estimation to obtain the modal data, and then rather than fitting the transformed nonlinear residual, one could fit the transformed version of the entire acceleration response. Although less conceptually appealing, because the response does not clearly consist of a nonlinear and a linear component, it might be slightly more efficient because the bases being used in the linear and the nonlinear fitting steps are not orthogonal to one another.

6. Summary and Conclusions

A general time-domain, least-squares based procedure is presented for analyzing dynamic response measurements from complex multi-degree-of-freedom nonlinear systems incorporating arbitrary types of nonlinear elements. The analysis procedure develops a reduced-order, nonlinear model whose format is convenient for numerical simulation studies. No information about the system's mass properties is needed, and only the applied excitations and corresponding response are needed to develop the model whose dimension is compatible with the number of available sensors. The utility of the approach is demonstrated by means of a three-degree-of-freedom system incorporating polynomial-type nonlinear features with hardening as well as softening characteristics.

Acknowledgments

This study was supported in part by grants from the Air Force Office of Scientific Research, the National Science Foundation, and the National Aeronautics and Space Administration.

References

1. Mohammad, K. S., Worden, K., and Tomlinson, G. R., 'Direct parameter estimation for linear and non-linear structures', *Journal of Sound and Vibration* **153**(3), 1992, 471–499.
2. Housner, G. W., Bergman, L. A., Caughey, T. K., Chassiakos, A. G., Claus, R. O., Masri, S. F., Skelton, R. E., Soong, T. T., Spencer, B. F., and Yao, J. T. P., 'Structural control: Past, present and future', *ASCE Journal of Engineering Mechanics* (Special Issue) **123**(9), 1997, 897–971.
3. Ghanem, R. and Romeo, F., 'A wavelet-based approach for model and parameter identification of nonlinear systems', *International Journal of Non-Linear Mechanics* **36**, 2001, 835–859.
4. Worden, K. and Tomlinson, G. R., *Nonlinearity in Structural Dynamics: Detection, Identification and Modelling*, Institute of Physics, London, 2001.
5. Vestroni, F. and Noori, M., 'Hysteresis in mechanical systems – modeling and dynamic response', Special Issue, *International Journal of Non-Linear Mechanics* **37**, 2002, 1261–1459.

6. Masri, S. F., Miller, R. K., Saud, A. F., and Caughey, T. K., 'Identification of nonlinear vibrating structures; Part I: Formulation', *ASME Journal of Applied Mechanics* **109**, December 1987, 918–922; "Part II: Applications', 923–929.
7. Worden, K., 'Data processing and experimental design for the restoring force method, Part I: Integration and differentiation of measured time data', *Mechanical Systems and Signal Processing* **4**, 1990, 295–319.
8. Smyth, A. W. and Pei, J.-S., 'Integration of measured response signals for nonlinear structural health monitoring', in *Proceedings of the 3rd US-Japan Workshop on Nonlinear System Identification and Health Monitoring,* Los Angeles, California, October 20–21, 2000.